Maura et al

“A practical guide for mutational signature analysis in hematological malignancies”

Supplementary Information

Supplementary Table 1. Summary of clinical and biological features of 30 multiple myeloma samples.

Sample ID	Age	Sex	Phase	Ig Type	Isotype	Cytogenetic
PD26400a	69	M	SMM	IgG	Kappa	HRD*
PD26401a	74	M	SMM	IgG	Kappa	
PD26402a	55	F	SMM	IgG	Kappa	t(11;14)
PD26403a	57	F	SMM	IgG	Kappa	HRD
PD26404a	64	M	SMM	IgG	Kappa	HRD
PD26405a	64	F	SMM	IgA	Kappa	t(4;14)
PD26406a	61	M	SMM	IgG	Kappa	t(4;14)
PD26407a	49	M	SMM	IgG	Kappa	HRD
PD26408a	53	M	SMM	IgG	Kappa	HRD
PD26409a	64	F	MGUS	IgG	Kappa	HRD
PD26410d	66	M	RR	IgG	Lambda	HRD
PD26411c	64	M	RR	IgA	Lambda	HRD
PD26412a	50	M	RR	IgG	Kappa	HRD
PD26414a	54	F	RR	IgA	Kappa	t(4;14)
PD26415c	55	M	RR	IgG	Kappa	HRD
PD26416d	52	F	RR	IgG	Kappa	HRD
PD26418a	71	M	RR	IgA	Kappa	t(11;14)
PD26419a	65	F	DG	LC	Kappa	t(8q24;14)
PD26420a	56	M	RR	IgM	Kappa	t(11;14)
PD26422d	70	M	RR	IgA	Kappa	t(11;14)
PD26423e	54	M	RR	IgG	Kappa	HRD
PD26424a	63	M	SMM	IgG	Kappa	HRD
PD26425e	63	M	RR	IgA	Kappa	t(11;14)
PD26426e	77	M	RR	IgG	Kappa	HRD
PD26427a	51	F	DG	LC	Lambda	t(11;14)
PD26428a	41	M	DG	IgG	Kappa	t(11;14)
PD26429a	64	F	DG	IgG	Kappa	HRD
PD26432c	61	M	RR	IgA	Lambda	HRD
PD26434c	58	M	DG	IgG	Kappa	t(11;14)
PD26435c	65	M	RR	IgA	Kappa	HRD

*HRD= hyperdiploid

Supplementary Figure 1. Mutational signature matrix decomposition. Schematic diagram explaining the mutational signature matrix decomposition according to the formula $C \approx SE$, where C is the catalogue matrix, with mutation types as rows and samples as columns, S is the signature matrix, with mutation types as rows and signatures as columns, and E is the exposure matrix, with signatures as rows and samples as columns.

$$C \approx SE$$

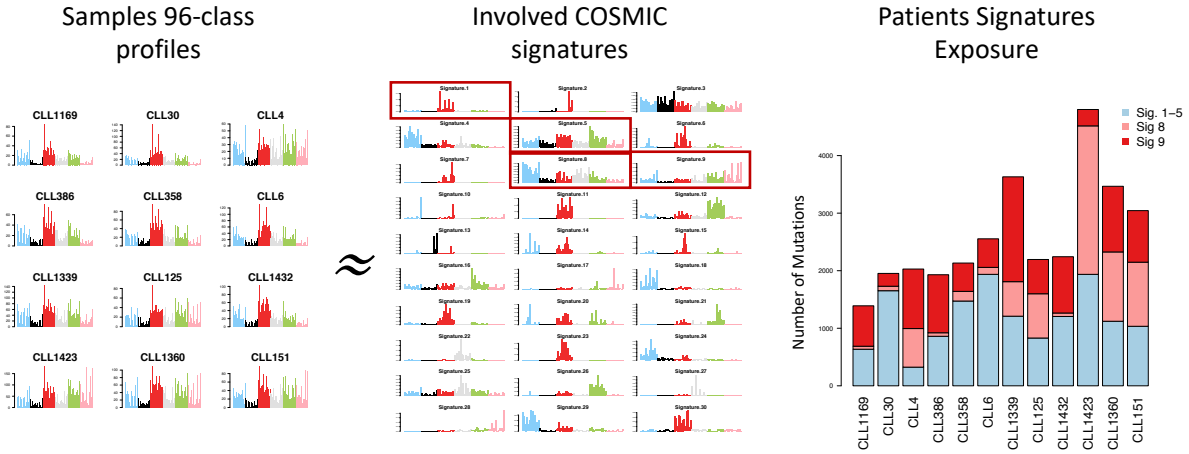

Supplementary Figure 2. Recurrent flat signatures in hematological cancers. The 96-mutational profile of Signature 3, 5 and 8, all considered as “flat” signatures due to the relatively even contribution of each trinucleotide context (<0.05).

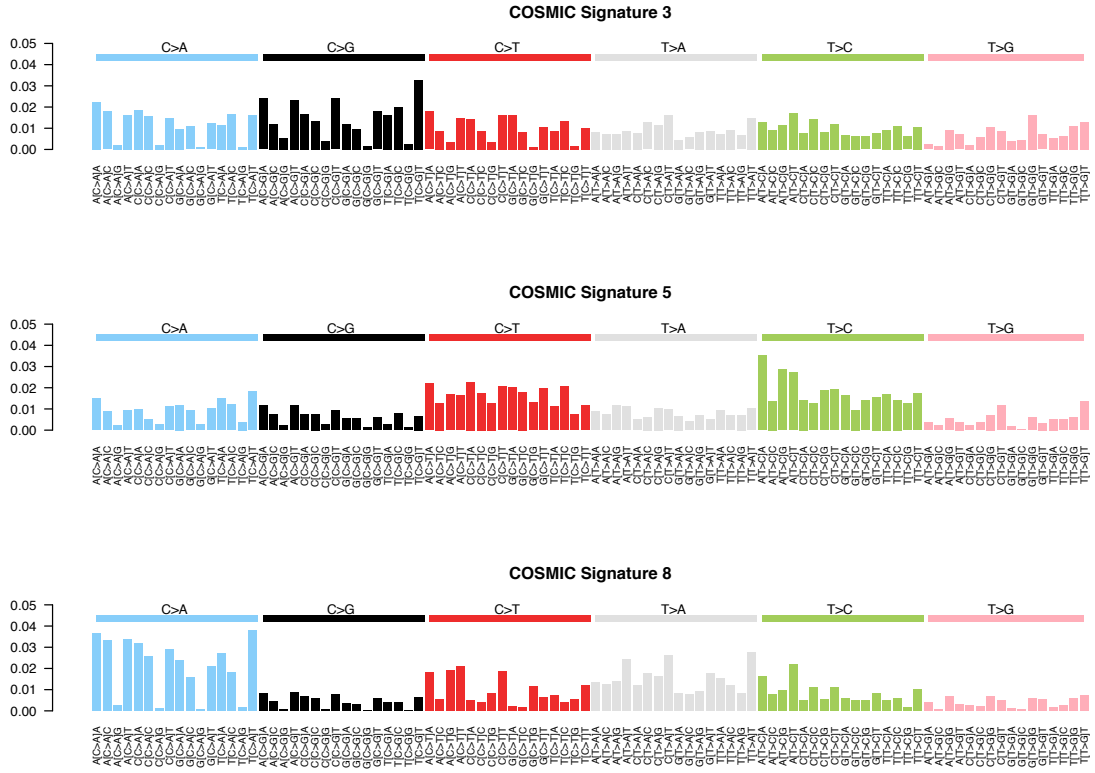

Supplementary Figure 3. Reconstruction error using MM mutational signatures. Reconstruction error of the 30 MM samples computed as KL divergence (KLD, top row), root mean squared error (RMSE, middle row) and cosine similarity (Cos Sim, bottom row), and using different combinations of the flat mutational signatures reported across different hematological malignancies (COSMIC Signatures 3, 5 and 8): including signature 3, 5 and 8 (with Sig. 3, 5 and 8), including only signatures 3 and 5 (without Sig. 8), including only signatures 5 and 8 (without Sig. 3), and including only signatures 3 and 8 (without Sig. 5). The first column (a,b,c) shows the reconstruction error in the three settings as boxplots, with p-values computed using a two-sided paired t-test; here, boxes show median, 1st and 3rd quartiles and whiskers are placed at the most external data point within 1.5*(75th-25th percentile). The second column (d,e,f) compares the reconstruction error in the setting “with Sig. 3 and 8” against “without Sig. 8”. The third column (g,h,i) compares “with Sig. 3, 5 and 8” against “without Sig. 3”; and the fourth column (j,k,l) compares “with Sig. 3, 5 and 8” against “without Sig. 5”. Black lines indicate the line $x = y$. The data point corresponding to sample PD26419a is marked with a red dot.

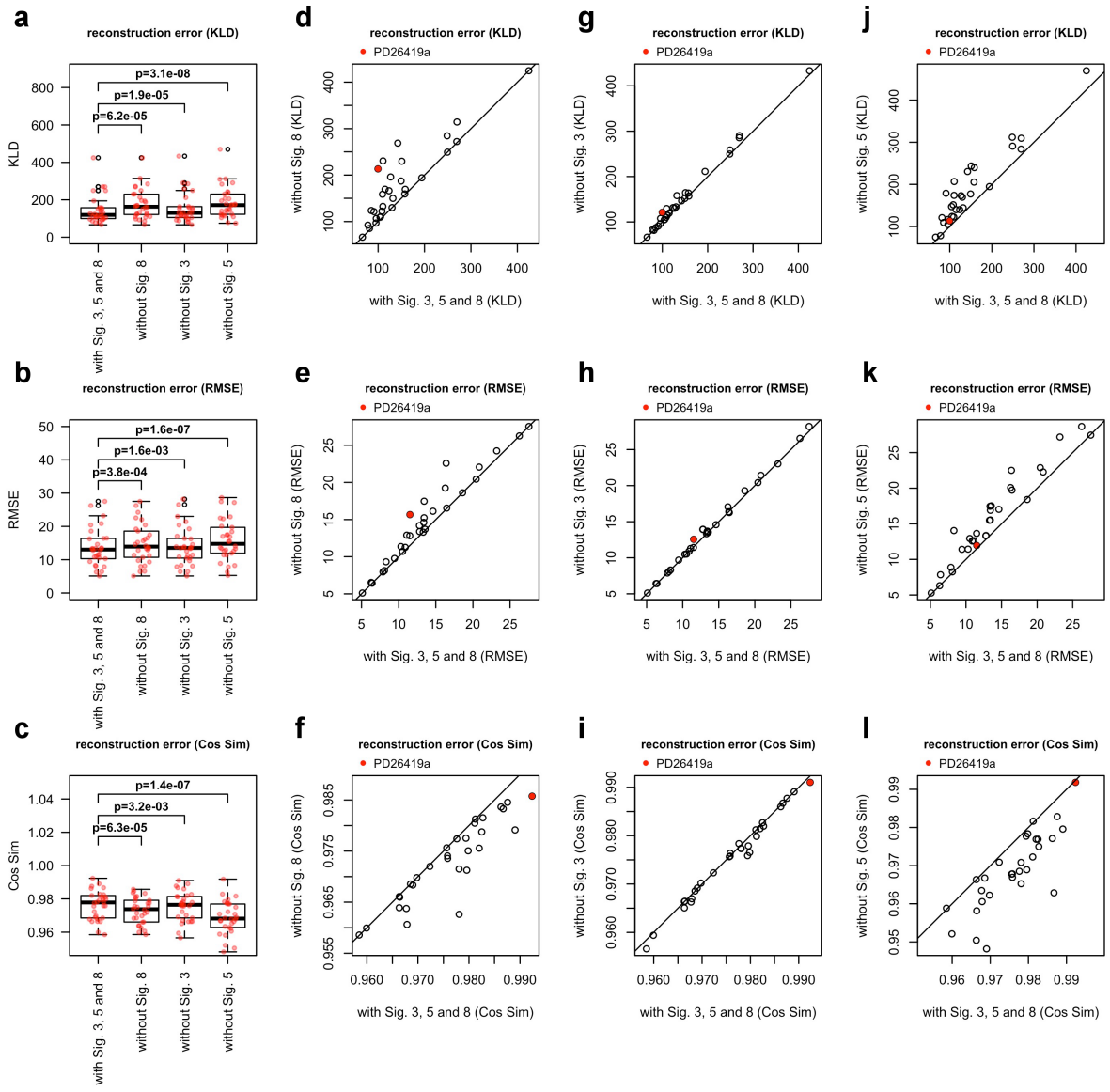
a
reconstruction error (KLD)
p=3.1e-08
p=1.9e-05
p=6.2e-05
KLD
with Sig. 3, 5 and 8
without Sig. 8
without Sig. 3
without Sig. 5
b
reconstruction error (RMSE)
p=1.6e-07
p=1.6e-03
p=3.8e-04
RMSE
c
reconstruction error (Cos Sim)
p=1.4e-07
p=3.2e-03
p=6.3e-05
Cos Sim
d
reconstruction error (KLD)
PD26419a
without Sig. 8 (KLD)
with Sig. 3, 5 and 8 (KLD)
e
reconstruction error (RMSE)
PD26419a
without Sig. 8 (RMSE)
with Sig. 3, 5 and 8 (RMSE)
f
reconstruction error (Cos Sim)
PD26419a
without Sig. 8 (Cos Sim)
with Sig. 3, 5 and 8 (Cos Sim)
g
reconstruction error (KLD)
PD26419a
without Sig. 3 (KLD)
with Sig. 3, 5 and 8 (KLD)
h
reconstruction error (RMSE)
PD26419a
without Sig. 3 (RMSE)
with Sig. 3, 5 and 8 (RMSE)
i
reconstruction error (Cos Sim)
PD26419a
without Sig. 3 (Cos Sim)
with Sig. 3, 5 and 8 (Cos Sim)
j
reconstruction error (KLD)
PD26419a
without Sig. 5 (KLD)
with Sig. 3, 5 and 8 (KLD)
k
reconstruction error (RMSE)
PD26419a
without Sig. 5 (RMSE)
with Sig. 3, 5 and 8 (RMSE)
l
reconstruction error (Cos Sim)
PD26419a
without Sig. 5 (Cos Sim)
with Sig. 3, 5 and 8 (Cos Sim)

Supplementary Figure 4. Mutational signature assignment in MM. Mutations assigned to signatures in the 30 MM samples, using different combinations of the mutational signatures 3 and 8: including only signature 8 (without Sig. 3), including both signatures 3 and 8 (with Sig. 3 and 8). Each dot is a sample. Black lines indicate the line $x = y$.

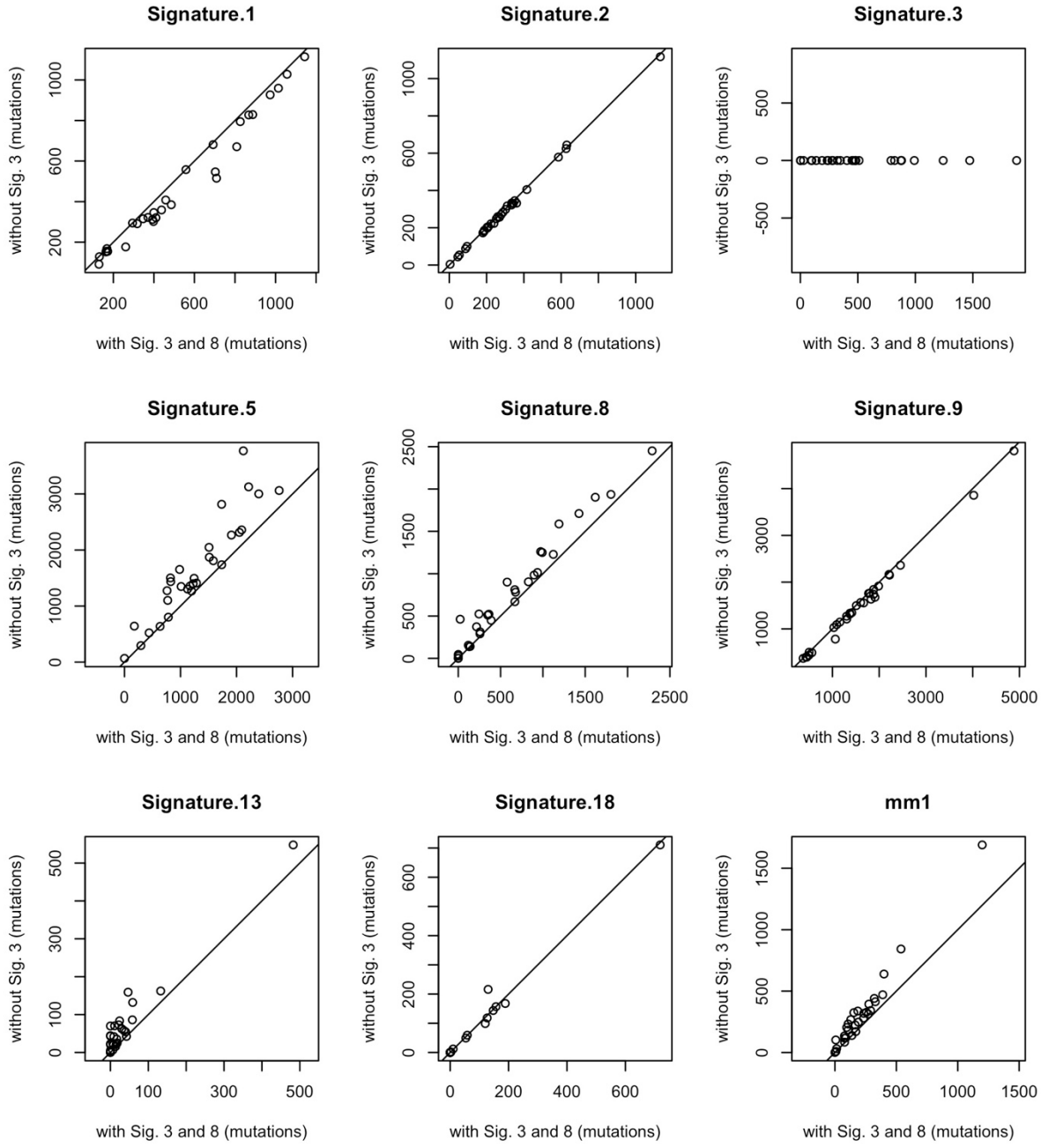

Supplementary Figure 5. Indel landscape in MM and BRCA-null breast cancer. We annotated the indel landscape according to the recently proposed classification [1] for all MMs (a), for PD26419a -the case that showed a uncertain HRD- (b) and for 2 BRCA-null breast cancers (c-d). In MMs and in PD26419a in particular we did not observe any enrichment for microhomology deletions as observed in the 2 BRCA1/BRCA2 deficient breast cancers.

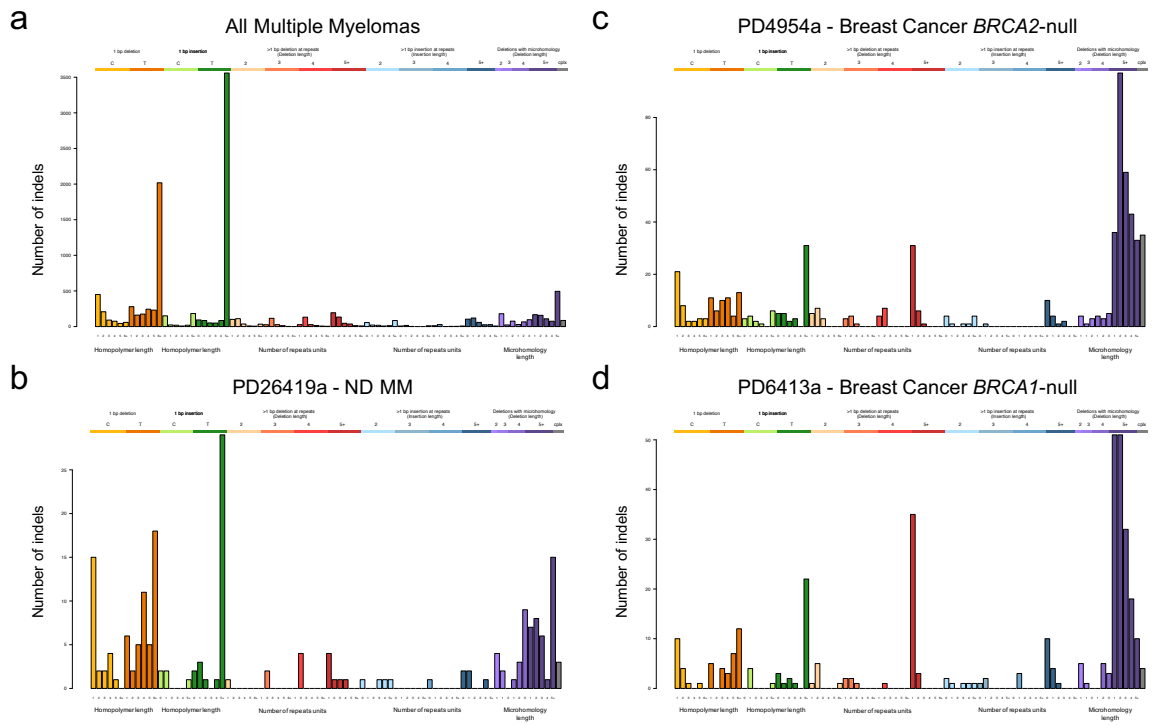

Supplementary Figure 6. The structural variant (SV) signatures for each MM case and for the 2 *BRCA*-null breast cancers. None of the MM samples had a SV signature profile similar to that observed among the *BRCA*-null breast cancers, that showed also a clear enrichment in term of SV prevalence.

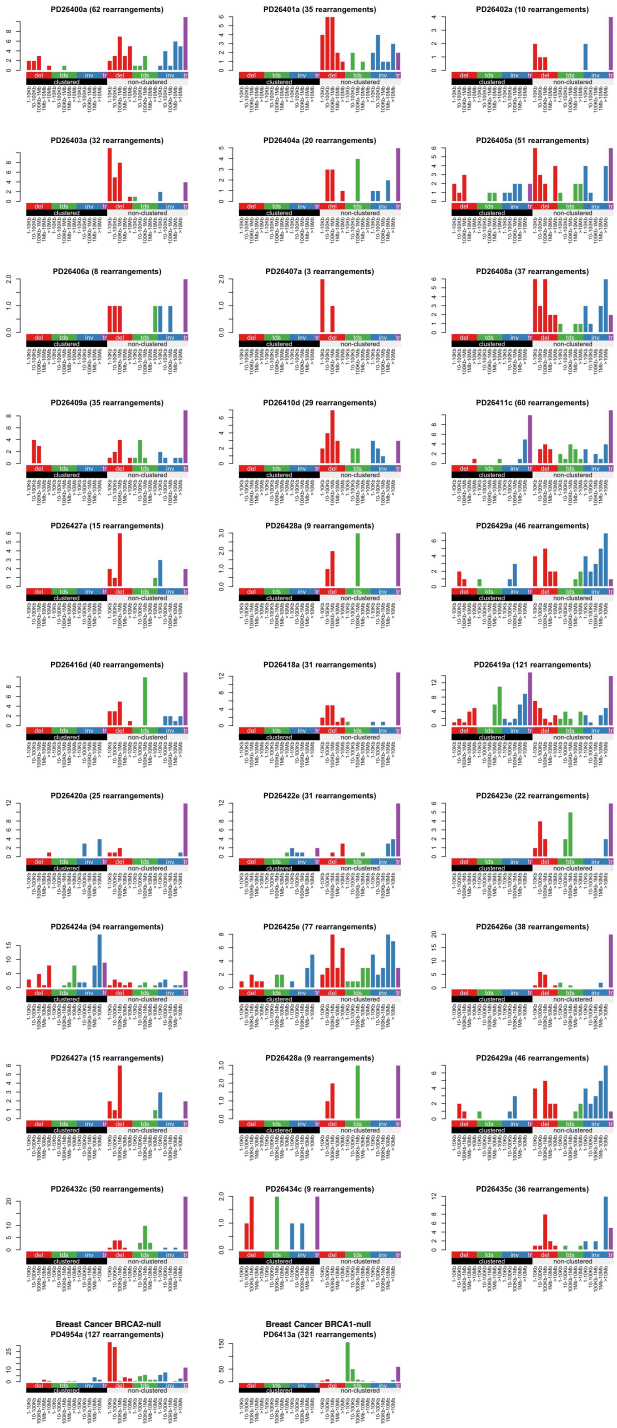

Supplementary Figure 7. AID mutational signatures. The 96-mutational profile of non-canonical AID (Signature 9, top) and canonical AID (bottom)[2,3]. The first is active all over the genome and represents one of the main mutational process in MM and M-CLL. Conversely, the second is active only as a localized mutational process within IGH/IGK/IGL regions and on few other off-target genes in cancer (i.e *BCL6*).

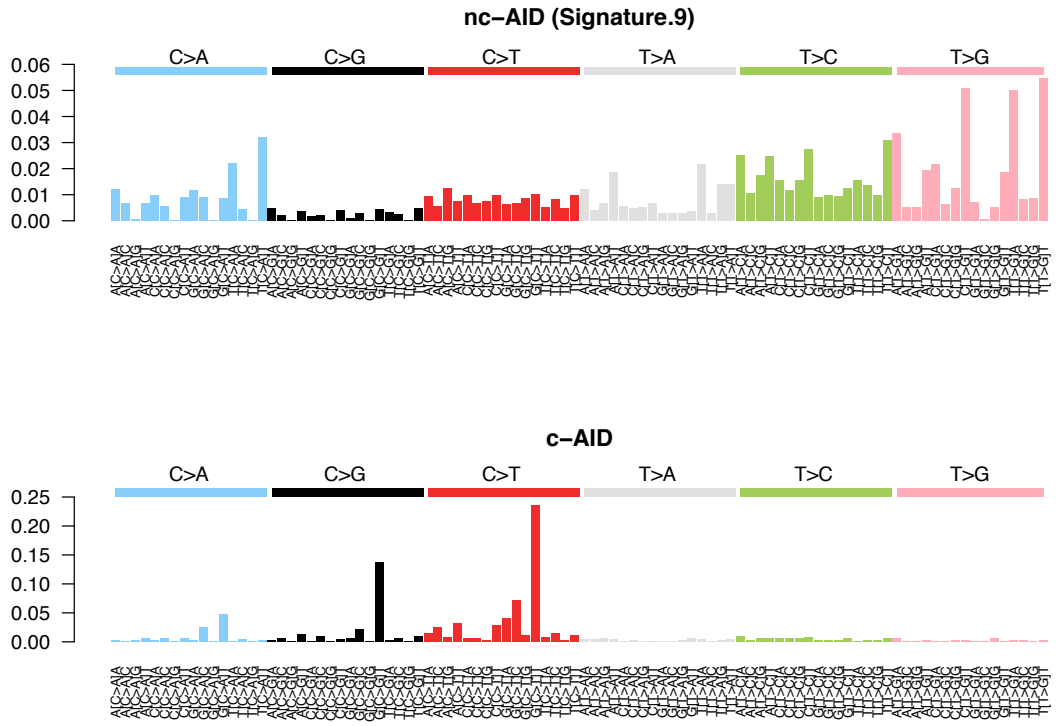

Supplementary Figure 8. CLL and MM mutation distribution on IGH. The SNV distribution on the IGH region of (a) M-CLLs (n=67), (b) U-CLLs (n=68) and (c) MMs (n=30). d) Relative and absolute mutation rate on coding gene within IGH locus. All cancers are subject to a different grade of c-AID activity, and, interestingly, in U-CLL cases this activity was mostly on the non-coding part compared to MM and M-CLL. e) The cancer cell fraction of all mutations within IGH/IGK/IGL loci. U-CLLs showed a significantly higher fraction of subclonal mutations compared to both M-CLL and MM ($p<0.0001$ and 0.01 respectively). P value were generated using the Wilcoxon test (R function wilcox.test)

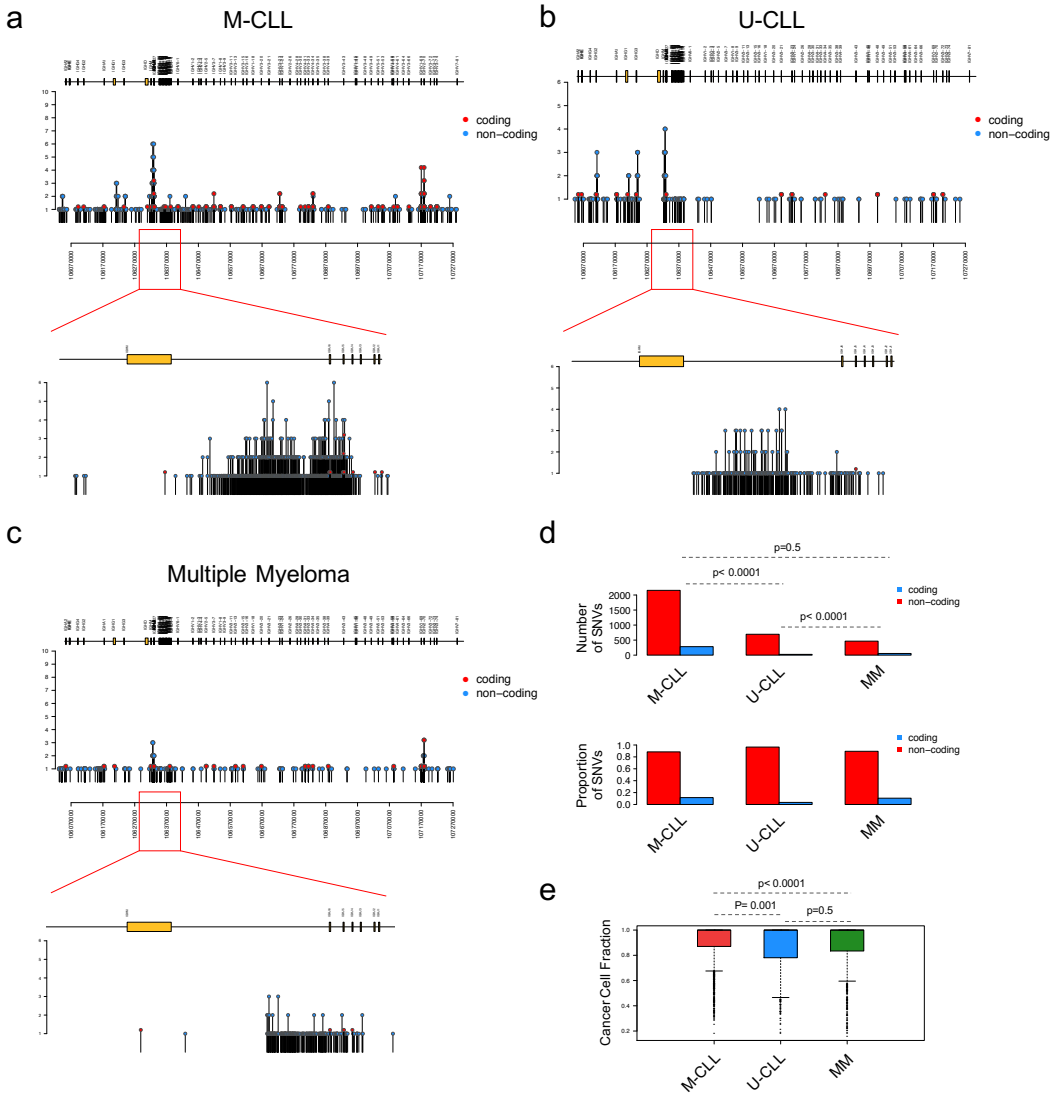

Supplementary Figure 9. Localized hypermutation on the IGH locus. In this cartoon, we summarized the VDJ recombination process. This recombination juxtaposes otherwise distant DNA segments, and once mapped to the germline reference genome the inter-mutational distance of c-AID localized hypermutation appears falsely high. The same rationale can be applied to other complex regions and events involving localized mutational events (i.e kataegis).

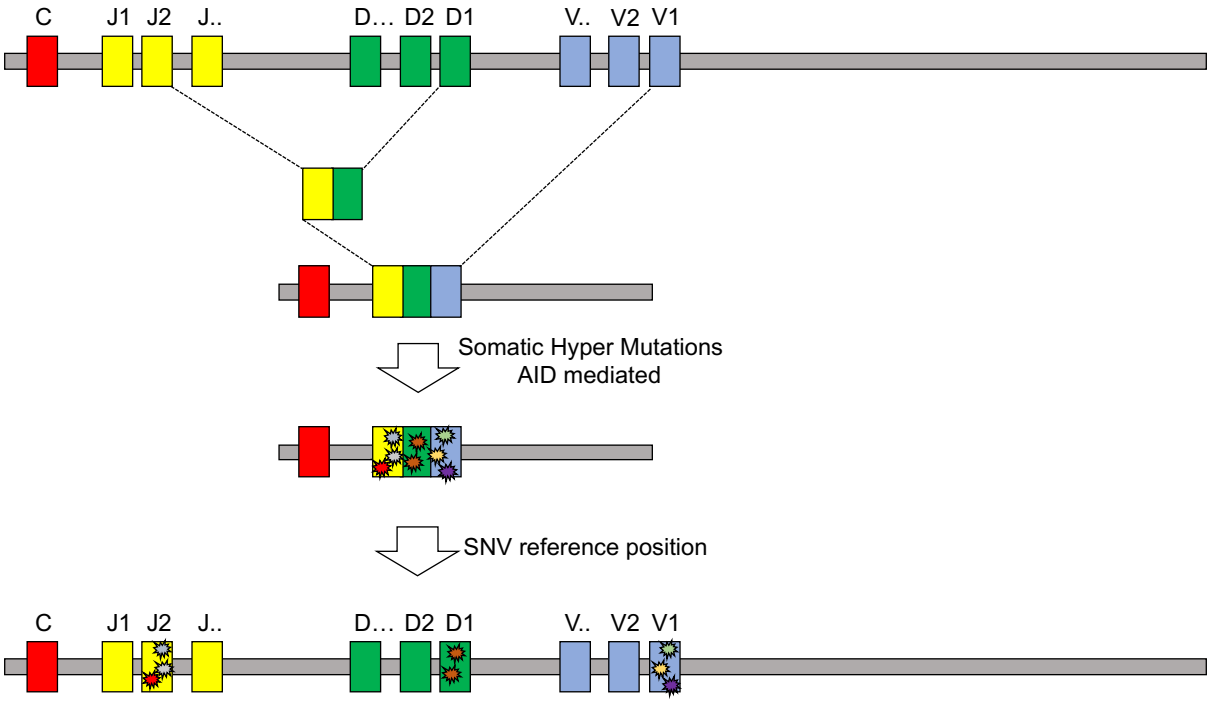

Supplementary Figure 10. BCL6 mutational distribution. a) distribution of SNVs within the *BCL6* gene locus for M-CLLs, U-CLLs and MMs. In contrast to the other entities, U-CLL did not show any evidence of localized hypermutation.

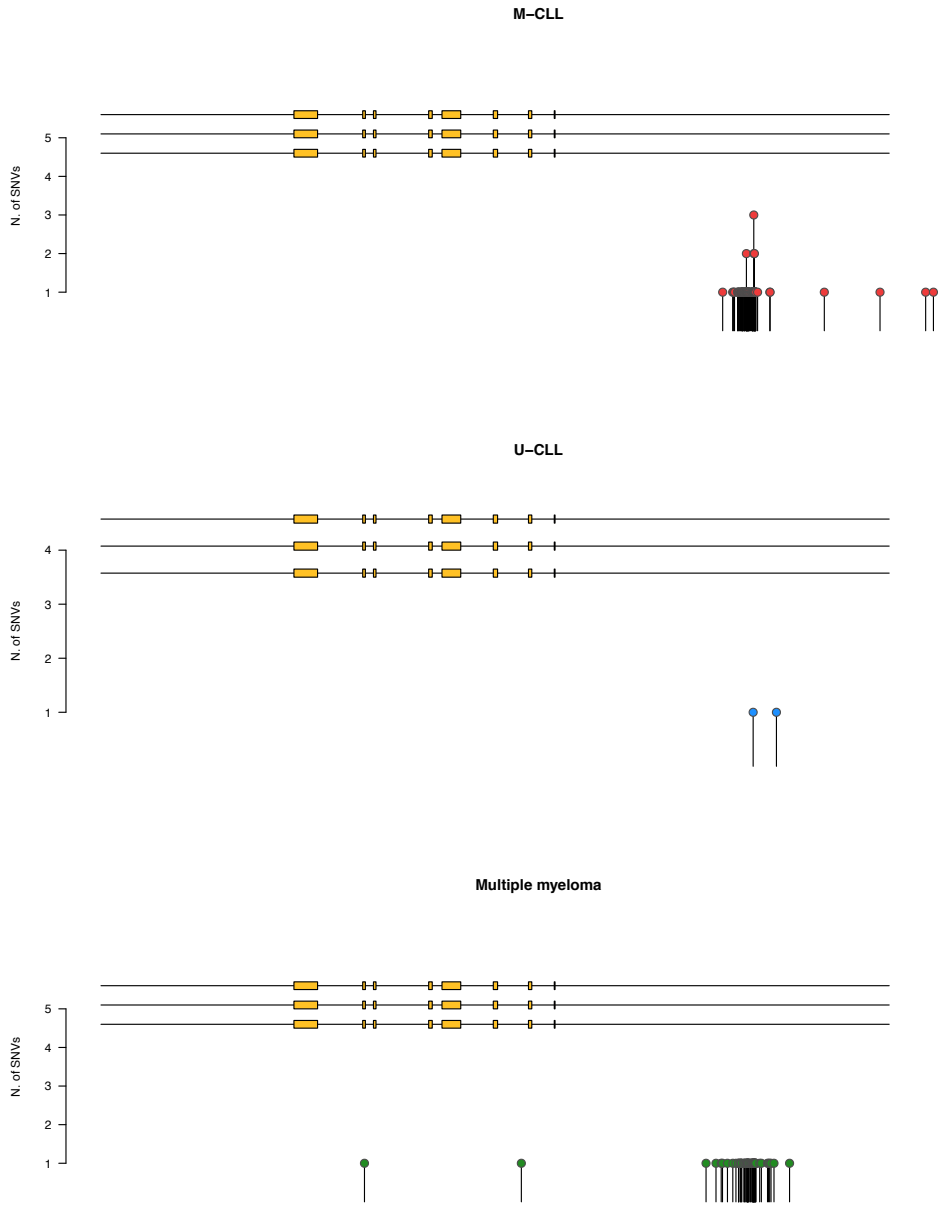

Supplementary Figure 11. Relative contribution of mutational signatures in CLL. Hierarchical clustering based on the relative contribution of each extracted mutational signature among 146 CLLs. Two main group are created, one with high and one with low signature 9 contribution. The first is mostly composed by M-CLL conversely the second grouped the great majority of U-CLL.

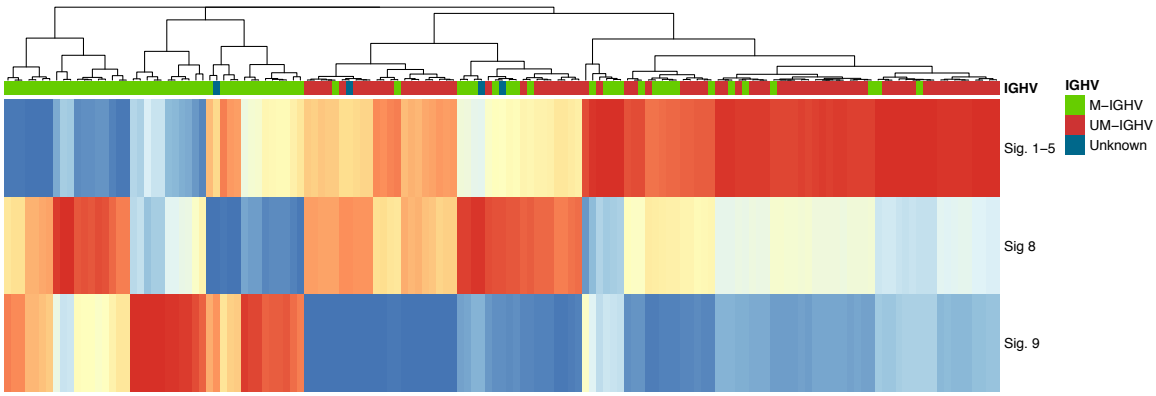

Supplementary Figure 12. The concordance rate between the published list of CLL variants on the IGH/IGK/IGL loci extracted by Sidron and the one extracted by 3 additional SNV callers (mutect2, caveman and muse).

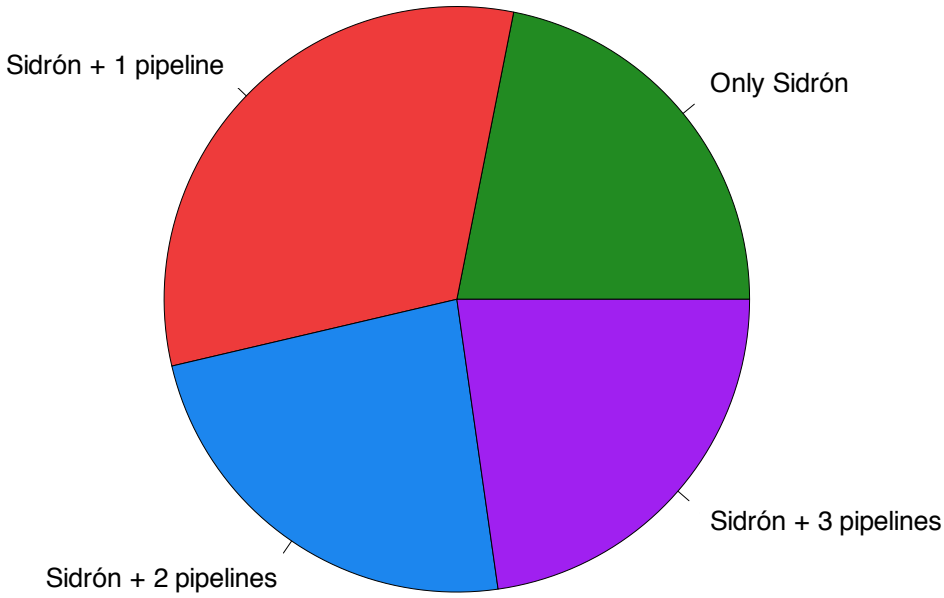

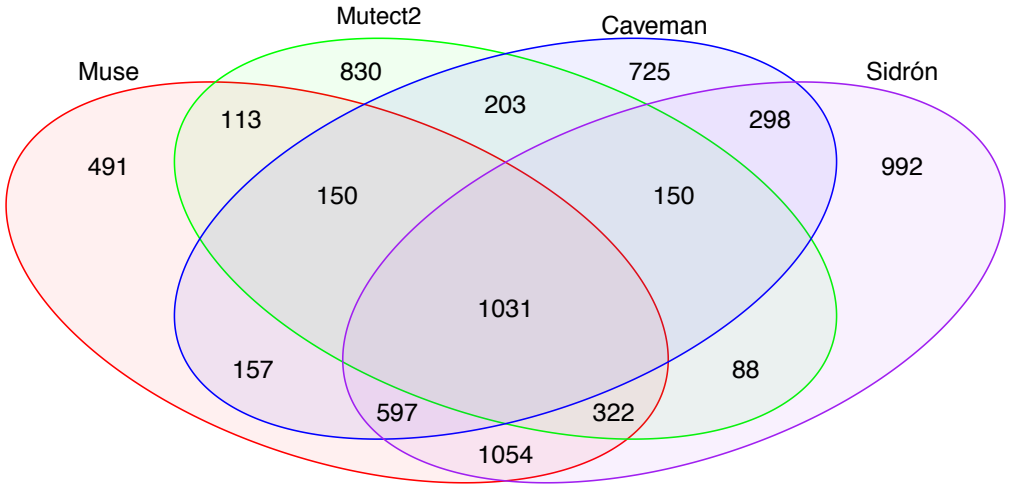

Supplementary References

1. Alexandrov, L.*, et al.* The Repertoire of Mutational Signatures in Human Cancer. Preprint at https://www.biorxiv.org/content/10.1101/322859v1 2018)

2. Bolli, N.*, et al.* Genomic patterns of progression in smoldering multiple myeloma. *Nat Commun* **9**, 3363 (2018).

3. Kasar, S.*, et al.* Whole-genome sequencing reveals activation-induced cytidine deaminase signatures during indolent chronic lymphocytic leukaemia evolution. *Nat Commun* **6**, 8866 (2015).